Parasitol Res (2003) 91: 215–228
DOI 10.1007/s00436-003-0948-9

ORIGINAL PAPER

Elizabeth G. Moodie · Leo F. Le Jambre
Margaret E. Katz

Thelohania montirivulorum sp. nov. (Microspora: Thelohaniidae), a parasite of the Australian freshwater crayfish, *Cherax destructor* (Decapoda: Parastacidae): fine ultrastructure, molecular characteristics and phylogenetic relationships

Received: 14 June 2003 / Accepted: 20 June 2003 / Published online: 16 August 2003

Abstract *Thelohania montirivulorum* sp. nov., a new species of microsporidian parasite, was found in a highland population of the Australian yabby, *Cherax destructor*. Data are presented on fine ultrastructure, developmental morphology and DNA sequence of the small subunit ribosomal DNA (SSU rDNA) and internal transcribed spacer region. The phylogenetic relationships of *T. montrivulorum* sp. nov. and other crayfish parasites in the genus *Thelohania*, based on the SSU rDNA sequence, are investigated. Fine ultrastructure, patterns of sporogony and SSU rDNA sequence similarities indicate *T. montirivulorum* sp. nov. is congeneric with *T. parastaci*, a parasite of lowland populations of *C. destructor*, and with *T. contejeani*, a parasite of European freshwater crayfish. SSU rDNA data suggests *Thelohania* species found in crustacean hosts are more closely related to the *Vairimorpha*/*Nosema* clade of species from insect and crustacean hosts than to the fire ant parasites, *T. solenopsae and Thelohania* sp.

Introduction

Thelohania Henneguy, 1892 (phylum Microspora) is a genus of intracellular parasites commonly reported to infect freshwater crayfish around the world (Sprague 1950; Cossins and Bowler 1974; Quilter 1976; France and Graham 1985; Lom et al. 2001). In Australia, the yabby, *Cherax destructor* (Clark, 1936) and related species in the family Parastacidae are parasitised (O'Donoghue and Adlard 2000). Surprisingly little is known about *Thelohania* species which infect Australian crayfish, given that infections may have significant pathogenic effects on economically important hosts and prevalences of infection of up to 30–40% have been reported in crayfish populations worldwide (O'Donoghue et al. 1990; Nylund and Westman 1992; Jones and Lawrence 2001). Muscle tissue is particularly targeted by *Thelohania*, with early stages of some species reported in the blood of the host (Sprague et al. 1992; Canning and Vavra 2000).

T. parastaci Moodie, 2002 is the first species of *Thelohania* to be described from an Australian crayfish host. It has been found in lowland populations of yabbies, including *C. destructor albidus* (Austin, 1996) from Western Australia and Victoria, and *C. d. rotundus* (Austin, 1996) from New South Wales (Austin 1996; Moodie et al. 2003). *T. parastaci* is very similar to the European crayfish parasite, *T. contejeani* Henneguy, 1892, which infects *Astacus fluviatilis* L. (Henneguy and Thelohan, 1892). Moodie et al. (2003) suggested a close relationship between the two species of *Thelohania* was indicated by features of their ultrastructure and development, and the relatively high sequence identity (92%) between the small subunit ribosomal DNA (SSU rDNA) sequences. The taxonomic affinities of *T. contejeani* have recently been reviewed in detail by Lom et al. (2001).

Recent studies, based on SSU rDNA sequences, have indicated that morphological and developmental life cycle features traditionally used in microsporidian taxonomy may not accurately reflect phylogenetic relationships between species (Weiss and Vossbrinck 1999). The type species for the genus *Thelohania* is *T. giardi* Henneguy, 1892, a parasite of the marine shrimp *Crangon crangon* (Linnaeus, 1758), synonymous with *C. vulgaris* Fabricius, 1798. Unfortunately, no molecular

E. G. Moodie (✉)
Zoology, School of Biological, Biomedical and Molecular Sciences, University of New England, NSW 2351, Armidale, Australia
E-mail: emoodie@pobox.une.edu.au

L. F. Le Jambre
CSIRO Livestock Industries,
Locked Bag 1, NSW 2350, Armidale, Australia

M. E. Katz
Molecular and Cellular Biology, School of Biological, Biomedical and Molecular Sciences, University of New England, NSW 2351, Armidale, Australia

data or information on fine ultrastructure is available for this species.

In this study, a second species of *Thelohania* which infects Australian freshwater crayfish is described, and the phylogenetic relationships between *Thelohania* species which parasitise crayfish, and a diverse sample of other microsporidians are investigated, based on SSU rDNA sequence comparisons. *T. montirivulorum* sp. nov., was discovered in a highland population of yabbies, *C. d. destructor* (Austin, 1996), in the headwaters of the Gwydir River in NSW, Australia. Morphological, ultrastructural and developmental characteristics are described, and SSU rDNA and internal transcribed spacer (ITS) region sequence data presented.

Materials and methods

Source of specimens

Heavily infected yabbies (*C. d. destructor*) were caught using dipnets and traps from Tea Tree Creek (30°30′S, 151°29′E) in the upper Gwydir River catchment on the New England Tableland, 20 km west of Armidale, NSW, Australia. Tissue samples from two adult female yabbies were processed for light microscopy, electron microscopy, DNA extraction, PCR amplification, cloning and sequencing of the SSU rDNA region, as described below.

Light microscopy

Microsporidian infection of yabbies was confirmed by examination of fresh squashes of anterior pleopod muscle at ×1,000 magnification under a Zeiss compound microscope. Impression smears of infected abdominal muscle were stained with 10% Giemsa (Undeen 1997). Semi-thin sections of tissue processed for electron microscopy (see below) were stained with 1% toluidine blue. Samples of fresh muscle tissue were stored frozen and later thawed for spores to be photographed and measured. Measurements were made using Photoshop 5.5 (Adobe, San Jose, Calif.) software.

Electron microscopy

Samples of fresh abdominal muscle, hepatopancreas, intestine and ovary were fixed overnight at 4°C in a mixture of 2% gluteraldehyde, 2% paraformaldehyde and 0.5% dimethyl sulfoxide in 0.1 M cacodylate buffer containing 8 mM $CaCl_2$ (J. Mathews, personal communication). Fixed tissues were washed five times in fresh 0.1 M cacodylate buffer and postfixed for 1–2 h in 1% osmium tetroxide. A 2% uranyl acetate bloc stain was performed at the second stage of dehydration through a graded acetone series. Tissue blocks were embedded in Spurr's resin. Ultrathin sections were post stained in uranyl acetate and lead citrate prior to examination with a Jeol JEM 1200 EX electron microscope, operated at 60 kV.

DNA extraction

Spores from approximately 0.5 g of heavily infected abdominal muscle were purified by digestion in 10 ml 2% pepsin (w/v) in 0.5% HCl (v/v) for 1 h at 37°C (Langdon 1991), pelleted by centrifugation at 1,800 *g* for 10 min and washed in sterile distilled water four times. The spore pellet was suspended in 50 µl extraction buffer (100 mM NaCl, 10 mM Tris-HCl, pH 8.0, 25 mM EDTA, 0.5% SDS), frozen and thawed three times, and then ground for 30 s in a 1.5-ml microfuge tube with a micropestle attached to a hand-held electric drill. A 450-ml volume of extraction buffer was added and the suspension incubated overnight at 37°C with proteinase K (200 µg per ml final concentration). The proteinase K was inactivated by heating the solution for 5 min at 95°C. After cooling to room temperature, the extract was incubated with RNase (100 µg per ml final concentration) for 30 min at 37°C.

Genomic DNA in the digestion solution was purified by extraction with phenol/chloroform/isoamyl alcohol (25:24:1), followed by extraction with chloroform/isoamyl alcohol (24:1). The purified DNA was precipitated with ethanol, dissolved in 100 µl TE buffer (10 mM Tris-HCl, pH 8.0, 1 mM EDTA) at 65°C for 1 h, and stored at –20°C. DNA concentration and purity was determined spectrophotometrically by measuring absorbance at wavelengths of 260 nm and 280 nm.

PCR amplification of SSU rDNA and the ITS region

The SSU rDNA of the microsporidian species under investigation was amplified by PCR, and then cloned prior to sequencing. Cloning was necessary because the primers used to amplify the SSU rDNA of *T. montirivulorum* sp. nov. also amplified the DNA of a second microsporidian species (*Vairimorpha* sp. AUS) that concurrently infected the host yabbies.

The universal primers 18f and 1492r (Weiss and Vossbrinck 1998) were used to amplify the SSU rDNA (Table 1). Each 50-µl PCR reaction mix contained 5 µl 10× reaction buffer without $MgCl_2$ (Promega, Madison, Wis.), 1.5 mM $MgCl_2$, 0.2 mM dNTPS, 25 pmol each primer, 1.25 units Taq DNA polymerase (Promega, Madison, Wis.) and 120 ng template DNA. PCR amplifications were performed as follows on a Mastercycler gradient thermocycler (Eppendorf, Hamburg, Germany): after an initial denaturation for 2 min at 94°C, samples were subjected to 35 cycles of amplification (denaturation at 94°C for 1 min, primer annealing at 48°C for 1 min, and extension at 68°C for 2 min), followed by a 10-min final extension at 68°C. A SSU fragment of 1,318 bp in length (including primers) was amplified and cloned as described below.

The ITS region, including the 3′ end of the SSU rRNA gene and the 5′ end of the large subunit (LSU) rRNA gene, was amplified with primers w1243f and BBAr (Table 1). These primers did not amplify DNA from *Vairimorpha* sp. AUS. In the same way as for amplification of the SSU rDNA, 50-µl reactions were prepared. PCR was performed under the same conditions, except that an annealing temperature of 50°C was used, and cyclic denaturation, annealing and extension times were reduced to 30 s, 30 s and 1 min respectively. A fragment of approximately 350 bp was amplified, purified with the Wizard PCR Preps Purification System (Promega, Madison, Wis.) and sequenced directly.

Table 1 Primers used to amplify and sequence rDNA of *Thelohania montirivulorum* sp. nov.

Primer	5′ → 3′ sequence	Melting temperature °C
SSU rDNA		
Forward		
18f	CACCAGGTTGATTCTGCC	56.0
w302f	GCGAAACTTACCCAATGCTA	61.5
T423f	GGCTTAATTTGACTCAACGC	58.0
Reverse		
1492r	GGTTACCTTGTTACGACTT	54.0
CP14r	CTGTTATCGCCCACTCCTTC	63.5
CP2r	TTCACCCCTCCCTATTTAATCC	63.7
ITS region		
Forward		
w1243f	GCCCGTCGTTATCTCAGATG	64.5
Reverse		
BBAr	TCCNRGTTRGTTTCTTTTCCT	61.0

Cloning

Purified PCR product (microsporidian SSU rDNA), from yabby Tx3, was ligated into a pGEM-T Easy plasmid vector (Promega, Madison, Wis.) and transformed into JM109 (Promega) competent cells. Plasmid DNA was purified from two clones that contained the SSU insert (A and D1) using a Wizard *Plus* Miniprep DNA purification kit (Promega) and sequenced.

Sequencing

Sequencing was performed by Newcastle DNA (University of Newcastle, NSW, Australia) using Big Dye Kit dye terminator chemistry and an automated ABI PRISM 377 DNA Sequencer (Applied Biosystems, Richmond, Va.). M13 forward and reverse primers (Promega, Madison, Wis.) were used to sequence the 5′ and 3′ ends of the SSU insert. The intervening portion of the SSU was sequenced with the internal primers w302f, T423f, CP14r and CP2r (Table 1). The ITS region was sequenced with primers w1243f and BBAr. Forward and reverse sequences were aligned with Clustal W Version1.82 (Thompson et al. 1994).

Phylogenetic analyses

Two groups of SSU rDNA sequences were aligned for phylogenetic analyses using Clustal X version 1.81 (Jeanmougin et al. 1998). The first group was aligned in order to examine the relationships between *Thelohania*, *Vairimorpha* and *Nosema* species that infect crustacean and insect hosts (Table 2). *Antonospora scoticae*, a distantly related microsporidian (Lom et al. 2001), was designated as the outgroup. The second alignment was performed in order to investigate relationships between *Thelohania* and other genera in a broader context, i.e. across the phylum Microspora. It comprised sequences from 56 taxa, including *Thelohania*, *Vairimorpha* and *Nosema*, and a wide spectrum of other microsporidian genera (Table 3). *Giardia lamblia* and *G. ardeae* were included as outgroup taxa.

Phylogenetic analyses were performed with PAUP* version 4.0b9 for Windows (Swofford 2000), and MrBayes (Huelsenbeck and Ronquist 2001) on an IBM-compatible personal computer (PC). Trees were constructed using neighbour-joining distance criteria, maximum parsimony criteria (branch and bound method for the smaller group, heuristic method for the larger group), and maximum likelihood criteria. Bootstrap values for the neighbour-joining and parsimony trees were calculated using 10,000 replicates. The optimum evolutionary model for maximum likelihood analyses was chosen using the program ModelTest 3.06 (Posada and Crandall 1998) with ancillary software, provided by Dr F.P. Patti (personal communication), to facilitate analysis on a PC.

When MrBayes analyses were performed, base frequencies, proportion of sites differing, transition to transversion ratios and the gamma-shape parameter were calculated from the data. For each MrBayes analysis, 1,000,000 iterations were carried out with 100 iterations per tree saved.

Results

T. montirivulorum sp. nov. is a dimorphic microsporidian with two simultaneous sporulation sequences in muscle tissue: one resulting in the formation of free binucleate spores, the other in the formation of eight uninucleate spores packaged within a sporophorous vesicle (SPV). Although mixed infections of *T. montirivulorum* sp. nov. and *Vairimorpha* sp. AUS in the same individual yabby were common, the different species could be distinguished on the basis of spore size and shape, arrangement of spores within sporophorous vesicles (SPVs), fine ultrastructure of spores and vesicles, and SSU rDNA sequence. Type specimens of *T. montivirulorum* sp. nov. were submitted to the Queensland Museum, Brisbane, Australia (registration numbers G463713 and G463714). Similarities and differences between *T. montirivulorum* sp. nov., *T. parastaci* and *T. contejeani* are discussed in the following text.

Table 2 GenBank accession numbers for 24 small subunit ribosomal DNA (SSU rDNA) sequences from *Thelohania*, *Nosema*, *Vairimorpha* and related species from arthropod hosts (*I* insect, *C* crustacean)

Organism	Host	GenBank accession no.
Microsporidium sp.	*Talorchestia deshayesei* (C)	AJ438963
Nosema apis	*Apis mellifera* (I)	X73894
Nosema bombycis	*Bombyx mori* (I)	D85504
Nosema ceranae	*Apis cerana* (I)	U26533
Nosema furnacalis	*Ostrinia furnacalis* (I)	U26532
Nosema granulosis	*Gammarus duebeni* (C)	AJ011833
Nosema oulemae	*Oulema melanopus* (I)	U27359
Nosema sp. NIS M11	*Bombyx mori* (I)	D85501
Nosema sp. SD NU	*Bombyx mori* (I)	D85503
Nosema trichoplusiae	*Apis cerana* (I)	U09282
Nosema tyriae	*Tyria jacobaeae* (I)	AJ012606
Nosema vespula	Unknown	U11047
Thelohania contejeani C2	*Astacus fluviatilis* (C)	AF492593
Thelohania montirivulorum sp. nov.	*Cherax destructor* (C)	AY183664
Thelohania parastaci	*Cherax destructor* (C)	AF294780
Thelohania solenopsae	*Solenopsis invicta* (I)	AF031538
Thelohania sp. FA	*Solenopsis richteri* (I)	AF031537
Vairimorpha imperfecta	*Plutella xylostella* (I)	AJ131645
Vairimorpha necatrix	*Pseudaletia unipuncta* (I)	Y00266
Vairimorpha sp. AUS	*Cherax destructor* (C)	AF327408
Vairimorpha sp. GER	*Plutella xylostella* (I)	AF124331
Vairimorpha sp. NIS M12	*Bombyx mori* (I)	D85502
Visvesvaria algerae[a]	Mosquito (I)	AF024656
Antonospora scoticae	*Andrena scotica* (I)	AF024655

[a] *Visvesvaria algerae* is synonymous with *Brachiola algerae*

Table 3 GenBank accession numbers for SSU rDNA sequences from 54 species of microsporidian and 2 species of *Giardia* (*I* insect, *C* crustacean, *A* annelid, *M*mammal, *F* fish, *B* bird)

Organism	Host	GenBank accession no.
Amblyospora californica	Mosquito (I)/copepod (C)	U68473
Amblyospora connecticus	Mosquito (I)/copepod (C)	AF025685
Amblyospora sp.	Mosquito (I)	U68474
Ameson michaelis	Decapod	L15741
Antonospora scoticae	Bee (I)	AF024655
Bacillidium sp.	Oligochaete (A)	AF104087
Culicosporella lunata	Mosquito (I)	AF027683
Edhazardia aedis	Mosquito (I)/copepod (C)	AF027684
Encephalitozoon cuniculi	Mammals (M)	L39107
Encephalitozoon hellem	Man (M)/bird (B)	L39108
Endoreticulatus schubergi	Moth (I)	L39109
Enterocytozoon bieneusi	Man (M)	L07123
Glugea anomala	Fish (F)	AF104084
Glugea atherinae	Fish (F)	U15987
Heterosporis sp. PF	Fish (F)	AF356225
Intrapredatorus barri	Mosquito (I)	AY013359
Janacekia debaesieuxi	Blackfly (I)	AJ252950
Kabatana takedai	Fish (F)	AF356222
Loma acerinae	Fish (F)	AF356224
Loma sp.	Fish (F)	AF104081
Microgemma sp.	Fish (F)	AJ252952
Microsporidium prosopium	Fish (F)	AF151529
Microsporidium sp.	Amphipod (C)	AJ438963
Nosema apis	Bee (I)	X73894
Nosema bombycis	Moth (I)	D85504
Nosema furnacalis	Beetle (I)	U26532
Nosema granulosis	Amphipod (C)	AJ011833
Nosema trichoplusiae	Bee (I)	U09282
Nucleospora salmonis	Fish (F)	U78176
Ovipleistophora mirandellae	Fish (F)	AF356223
Parathelohania anophelis	Mosquito (I)	AF027682
Pleistophora ovariae	Fish (F)	AJ252955
Pleistophora sp. 3	Fish (F)	AF104082
Pleistophora sp. A	Insect (I)	U10342
Pleistophora sp. LS	Decapod (C)	AJ252959
Pleistophora sp. PA	Decapod (C)	AJ252958
Pleistophora typicalis	Fish (F)	AF104080
Polydispyrenia simulii	Blackfly (I)	AJ252960
Septata intestinalis	Man (M)	L39113
Spraguea lophii	Fish (F)	AF104086
Thelohania contejeani C2	Crayfish (C)	AF492593
Thelohania montirivulorum sp. n.	Crayfish (C)	AY183664
Thelohania parastaci	Crayfish (C)	AF294780
Thelohania solenopsae	Ant (I)	AF031538
Trachipleistophora hominis	Man (M)	AJ002605
Vairimorpha imperfecta	Moth (I)	AJ131645
Vairimorpha necatrix	Moth (I)	Y00266
Vairimorpha sp. AUS	Crayfish (C)	AF327408
Vavraia culicis	Mosquito (I)	AJ252961
Vavraia oncoperae	Caterpillar (I)	X74112
Visvesvaria acridophagus	Mosquito (I)	AF024658
Visvesvaria algerae	Mosquito (I)	AF024656
Vittaforma corneae	Man (M)	L39112
Weiseria palustris	Blackfly (I)	AF132544
Giardia ardeae	Birds (A)	Z17210
Giardia lamblia	Mammals (M)	M54878

Light microscopy

Binucleate single spores (Fig. 1) and uninucleate spores within SPVs (Figs. 2, 3) were found together in high numbers in myocytes in the abdomen and appendages of infected crayfish. Binucleate spores were highly variable in size and often appeared imperfectly formed. The number of spores within the sporophorous vesicles (SPVs) varied from two to eight. Groups of three, four and six spores were common. Freshly thawed spores averaged 5.9×2.6 μm in diameter (n =40). SPVs averaged 8.4 μm in diameter (n =20). The average dimensions of spores, vesicles and internal structures, from *T. montirivulorum* sp. nov., *T. parastaci* and *T. contejeani,* are compared in Table 4.

Electron microscopy

Sporonts

Early meronts were not observed in the heavily infected crayfish that were sampled. Diplokaryotic sporonts gave rise to both binucleate spores and uninucleate spores in SPVs. A single early sporont with two pairs of diplokaryotic nuclei, surrounded by ribbons of ribosomes, is shown in Fig. 4. It is presumably undergoing binary fission, and cytokinesis has not yet occurred. Only one type of sporont was observed. Sporonts were characterised by highly vesicular cytoplasm and thickening of the external sporont membrane with electron-dense material (Fig. 5). SPV formation was observed around some sporonts (Figs. 6, 7) prior to the division of the binucleate sporont into two to eight uninucleate sporoblasts.

Sporophorous vesicles

The ultrastructural features of the episporontal space in SPVs were very similar to those described for *T. parastaci* (Moodie et al. 2003) and *T. contejeani* (Lom et al. 2001). Macrotubules (average diameter: 171 nm, $n = 60$) and microtubules (average diameter: 85 nm, $n = 60$) were evident in the cytoplasm external to the developing sporoblasts (Figs. 8, 9). The macrotubules appeared to be composed of coiled stacks of fibres. Aggregations of granules (dense bodies) were evident within SPVs external to early sporoblasts. The size of the dense body was inversely related to the number of free microtubules in the SPV. As the sporoblasts matured, they acquired a halo of microtubules, and fine filamentous projections from the exospore coat into the episporontal space were evident (Fig. 9).

Sporoblast development

Within SPVs, separation of the sporoblast nuclei preceded division of the rosette-shaped plasmodium into individual uninucleate cells. Two sporoblasts, which have not yet separated from the plasmodium, can be seen in Fig. 10. Mature sporoblasts were characterised by relatively thick deposits of electron-dense material on the outside of the plasmalemma, the developing exospore coat. In fully mature spores, an electron-lucent endospore layer between the exospore and the plasmalemma was clearly visible (Fig. 9).

Mature uninucleate spores

Uninucleate spores were produced only within SPVs. The polar filament was isofilar and coiled 20–22 times, adjacent to the posterior vacuole (Fig. 11). The average diameter of the polar filament was 98 nm ($n = 89$). Dimensions of fresh uninucleate spores could not be measured accurately within vesicles, although they appeared similar to binucleate spores (Figs. 1, 2). Lateral exospore and endospore widths were 30–40 nm and 80–130 nm, respectively ($n = 9$). The spore coat was thicker in uninucleate spores than in binucleate spores (Table 4).

Mature binucleate spores

Binucleate spores were in direct contact with host cell cytoplasm. Immature spores (Fig. 12) showed fewer coils of the polar filament than mature spores (Fig. 13). The isofilar polar filament, adjacent to the posterior vacuole, was coiled 20–22 times in mature spores. Microtubules were visible in close proximity to the exospore coat (Fig. 13). Lateral exospore and endospore widths in binucleate spores were 17–30 nm and 40–80 nm, respectively ($n = 8$). The average diameter of the polar filament was 107 nm ($n = 74$). Some mature spores had a crenellated appearance, possibly a fixation artifact (Fig. 14).

The anterior polaroplast was a crescent-shaped structure consisting of parallel, narrowly spaced lamellae, which stained darkly. The lamellae in the posterior polaroplast were more widely spaced and irregular in orientation, and took up stain less readily (Fig. 15). The manubrium, or anterior section of the polar filament, bisected the polaroplast as it descended toward the posterior vacuole from the polar capsule and anchoring disc. No filamentous projections from the exospore layer were seen in sections of diplokaryotic spores.

Tissue tropism

T. montirivulorum sp. nov. showed marked muscle tissue tropism. No stages were found within haemocytes in the hepatopancreas, although only a small number of sections containing haemocytes were examined.

SSU and ITS ribosomal DNA sequences

Identical SSU rDNA sequences were obtained from clones A and D1 of *T. montirivulorum* sp. nov. from yabby Tx3. The SSU rDNA sequence from clone A, excluding the external 18f and 1492r primers, was submitted to GenBank (accession no. AY183664). The SSU rDNA gene was 1,318-bp long, including the 18f and 1492r primers. This compared with 1,337 bp for *T. parastaci* (Moodie et al. 2003) and 1,361 bp for *T. contejeani* c2 (Lom et al. 2001). *T. montirivulorum* sp. nov. showed 93% sequence identity with *T. parastaci* and 91% sequence identity with *T. contejeani* c2.

Sequence of the ITS region of the rDNA from *T. montirivulorum* sp. nov. was submitted to GenBank (accession no. AY183665). The ITS region of *T. montirivulorum* sp.nov. was significantly different to that of

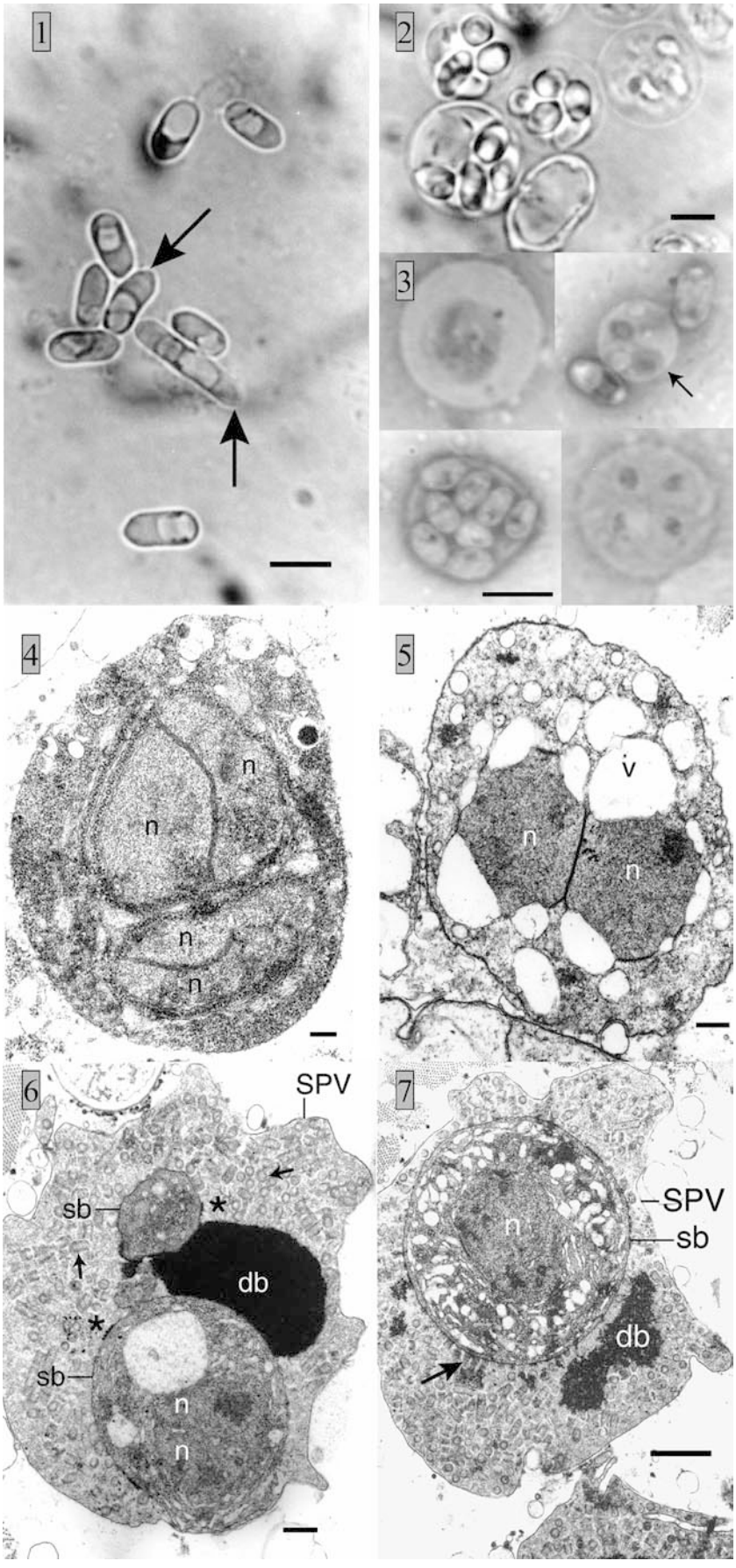

Fig. 1 *T. montirivulorum* sp. nov., light micrograph of fresh binucleate spores, some malformed (*arrows*). *Scale bar* 5 μm

Fig. 2 Light micrograph of sporophorous vesicles (*SPVs*) containing variable numbers of spores. *Scale bar* 5 μm

Fig. 3 Light micrograph of Giemsa-stained SPVs, with one and two nuclei (*arrow*), four and eight cells (*clockwise from top left*). *Scale bar* 5 μm

Fig. 4 Sporont undergoing binary fission. Pairs of diplokaryotic nuclei (*n*) have separated prior to division of the cytoplasm. *Scale bar* 200 nm

Fig. 5 Diplokaryotic sporont with many vesicles (*v*) in the cytoplasm and adjacent to the nuclei (*n*). *Scale bar* 500 μm

Fig. 6 Sporophorous vesicle (*SPV*) containing a sporont/sporoblast transitional stage (*sb*) and a dense body (*db*). The nuclei (*n*) in the lower sporoblast have not yet separated. There are numerous macrotubules (*arrows*) in SPV and aggregations of microtubules (*) on sporoblast walls. *Scale bar* 500 nm

Fig. 7 Sporophorous vesicle (*SPV*) containing a sporont/sporoblast transitional stage (*sb*) with condensed nuclear material at opposite poles of the nucleus (*n*), and a granular dense body (*db*). Numerous macrotubules (*arrow*) are visible adhering to the sporoblast wall and in the SPV cytoplasm. *Scale bar* 1 μm

Table 4 Comparison of morphological features of *T. montirivulorum* sp. nov.,*T. parastaci* and *T. contejeani*

Feature	*T. montirivulus* sp. n.	*T. parastaci* (Moodie et al., in preparation)	*T. contejeani* (Lom et al. 2001)
Spore shape	Lozenge, rounded ends	Lozenge, rounded ends	Oval, wider posterior end
Fresh binucleate spore length (μm)	5.9 (4.9–7.2)	3.9 (3.2–4.9)	3.8
Fresh binucleate spore width (μm)	2.6 (2.0–3.1)	2.0 (1.5–2.7)	1.8
Polaroplast morphology (anterior/posterior)	Lamellar/lamellar	Lamellar/lamellar	Lamellar/lamellar
Binucleate spore—no. coils in polar filament	20–22	6–8	5–7
Polar filament diameter (nm)	107 (90–140)	83 (65–102)	
Uninucleate spore—no. coils in polar filament	20–22	11–20	9–10
Polar filament diameter (nm)	98 (82–111)	59 (53–74)	120–180 [a]
SPV diameter (μm)	8.4 (7.0–9.6)	8.8 (7.4–10.5)	8–9 [a]
SPV macrotubule diameter (nm)	171 (130–249)	249 (205–307)	220
SPV microtubule diameter (nm)	85 (63–117)	73 (50–99)	80–100
Lateral exospore thickness of binucleate spores (nm)	22 (17–30)	34 (30–40)	Not measured
Lateral endospore thickness of binucleate spores (nm)	65 (40–80)	58 (50–60)	Not measured
Lateral exospore thickness of uninucleate spores (nm)	31 (30–40)	24 (20–40)	24–30 [b] only uninucleate spores reported
Lateral endospore thickness of uninucleate spores (nm)	108 (80–130)	73 (56–110)	60–90 [b] only uninucleate spores reported

[a]Cossins 1974
[b]Vivares 1975

T. parastaci. The two species showed 76% identity across 196 bases immediately downstream of the 1492r primer.

Phylogenetic analyses based on SSU rDNA

Relationships between species in the genera *Thelohania*, *Vairimorpha* and *Nosema* are described in Fig. 16. The relationships between the above taxa and 41 other microsporidian genera as determined by distance, parsimony and maximum likelihood criteria (MrBayes) are described in Figs. 17, 18 and 19. The General Time Reversible model with rate heterogeneity (Lanave et al. 1984; Rodriguez et al. 1990) was determined by Modeltest to be the optimal evolutionary model for phylogenetic tree construction, based on the SSU rDNA data used. The GTR + G model was determined to be optimal for the smaller analysis (Fig. 16C), whereas the GTR + G + I model was the best available for the larger analysis (Fig. 19). In all trees, irrespective of the method of analysis, the three crayfish parasites: *T. montirivulorum* sp. nov., *T. parastaci*, and *T. contejeani*, were placed together in a clade with *Microsporidium* sp., a parasite of a marine amphipod. This clade was a sister to the *Vairimorpha*/*Nosema* clade (Fig. 16), which included *Vairimorpha* sp. AUS, a parasite of the same yabbies in which *T. montirivulorum* sp. nov. was found.

The relationships between the two Australian species, *T. montirivulorum* sp. nov. and *T. parastaci,* and the European crayfish pathogen, *T. contejeani*, varied depending on the number of taxa included in the analysis and the criteria used to construct the phylogenetic trees. Bootstrap values of less than 95% are thought to indicate that the branching pattern on a tree may not be well supported (Page and Holmes 1998). The bipartitioning of *T. parastaci* with *T. montirivulorum* sp. nov. rather than with *T. contejeani* is well supported in the distance tree from the analysis of the smaller group of genera (Fig. 16A) and in the Bayesian maximum likelihood tree from the analysis of the larger group of genera (Fig. 19). In all other trees, the precise nature of the relationships between these three species was unresolved, as indicated by the relatively low bootstrap values (Figs. 16B, 17, 18) or frequency of observed bipartitions (Fig. 16C) at the relevant nodes.

The fire ant parasites, *T. solenopsae* and *Thelohania* sp. FA, were invariably assigned to the same clade as *Visvesvaria algerae* (synonymous with *Brachiola algerae*), outside both the crustacean *Thelohania* clade and the *Vairimorpha*/*Nosema* clade. In the Bayesian tree generated by analysis of the larger group of microsporidian genera (Fig. 19) *T. solenopsae* was placed in a more basal position with respect to the crustacean *Thelohania* clade than did trees generated by distance or parsimony criteria (Figs. 17, 18). With some exceptions, grouping of microsporidians on branches in the Bayesian tree correlated with broad host taxa, e.g. insects, mammals, fish, crustaceans (Fig. 19). The relatively low bootstrap values for the more internal nodes in the distance and parsimony trees in Figs. 17 and 18 indicate that the data available is insufficient to resolve relationships at these levels.

Discussion

Ultrastructural, developmental, and SSU rDNA sequence similarities between *T. montirivulorum* sp. nov., *T. parastaci* and *T. contejeani* justified the inclusion of this new species in the same genus. Shared features include the presence of characteristic macrotubules,

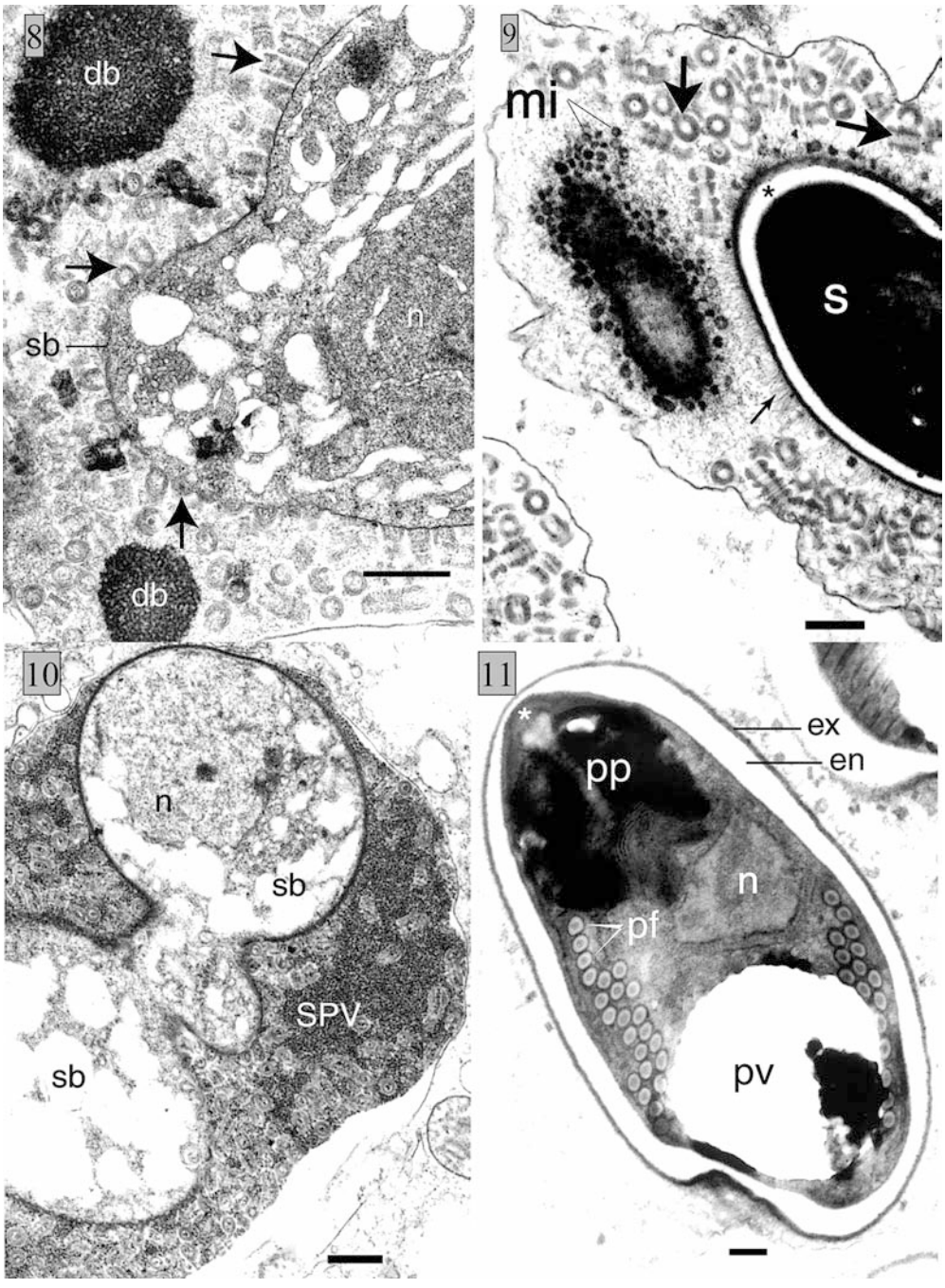

Fig. 8 SPV with macrotubules (*arrows*) attached to the external sporoblast wall and free in the cytoplasm. Two granular dense bodies (*db*) are apparent in the SPV. *Scale bar* 500 nm

Fig. 9 SPV with macrotubules (*large arrows*), microtubules (*mi*) and fine filamentous projections (*small arrow*) extending out from the spore (*s*). An electron-lucent endospore (*) is clearly visible. *Scale bar* 500 nm

Fig. 10 Dividing sporoblasts (*sb*) within a SPV. Note the single nucleus (*n*) and very granular cytoplasm in the SPV. *Scale bar* 500 nm

Fig. 11 Mature uninucleate spore from within an SPV. Anchoring disc (*), polaroplast (*pp*), exospore (*ex*), endospore (*en*), single nucleus (*n*), large posterior vacuole (*pv*), and 22 coils of the polar filament (*pf*) are visible. *Scale bar* 200 nm

microtubules, and dense bodies in sporophorous vesicles, development of up to eight uninucleate sporoblasts from a rosette-shaped plasmodium within the SPV, formation of binucleate (diplokaryotic) sporonts, simultaneous dimorphic sporogony resulting in binucleate and uninucleate spores, marked muscle tissue tropism and common host taxa (Decapoda: Astacidea). The formation of uninucleate spores is presumed to involve meiosis (Flegel and Pasharawipas 1995; Lom et al. 2001).

T. montirivulorum sp. nov. could be differentiated from *T. parastaci* and *T. contejeani* by differences in SSU rDNA sequence, variable dimensions of the relatively large spores of *T. montirivulorum* sp. nov. and the variable number of spores in each SPV, and the higher number of coils of the polar filament in binucleate spores of *T. monirivulorum* sp. nov. in comparison to the other species (Table 4).

In a review of the taxonomic affinities of *T. contejeani*, Lom et al. (2001) concluded that dimorphic sporogony of *T. contejeani* precluded it from sharing congeneric status with the marine decapod parasites, *T. maenadis* Perez, 1904, or *T. octospora* Henneguy, 1892 (Vivares 1975, 1980), for which only monomorphic sporogony had been described. For the same reasons, *T. contejeani* could not be included in the family

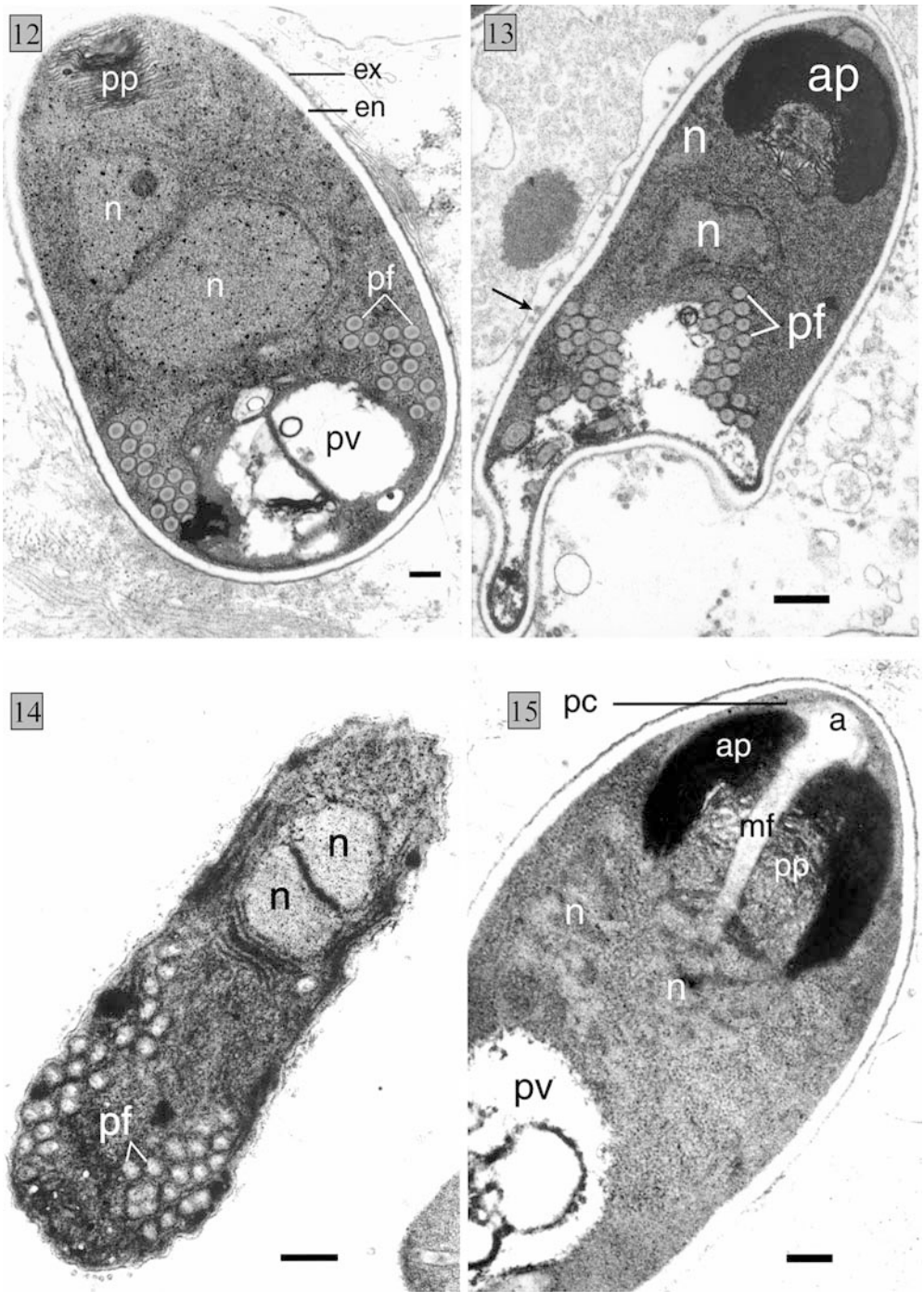

Fig. 12 Binucleate (*n*) late sporoblast showing rudimentary polaroplast (*pp*) and 14 coils of polar filament (*pf*) adjacent to posterior vacuole (*pv*). Exospore (*ex*) and endospore (*en*) layers are well developed. *Scale bar* 200 nm

Fig. 13 Mature binucleate (*n*) spore with darkly stained anterior polaroplast (*ap*) cupped around the posterior polaroplast, and 22 coils of the polar filament adjacent to the posterior vacuole. Microtubules (*arrow*) can be seen in close proximity to the spore wall. *Scale bar* 500 nm

Fig. 14 Spore with diplokaryotic nuclei (*n*) and 20 coils of the polar filament (*pf*). Note the crenellated spore wall. *Scale bar* 500 nm

Fig. 15 Mature binucleate spore showing crescent-shaped anterior polaroplast (*ap*), cupped around the posterior polaroplast (*pp*), and the manubrium of the polar filament (*mf*) descending from the anchoring disc (*a*) within a polar capsule (*pc*). Ribbons of ribosomes surround the nuclei (*n*). The posterior vacuole (*pv*) is visible. *Scale bar* 200 nm

Thelohaniidae or the superfamily Thelohanoidea, which are monomorphic as strictly defined by Sprague et al. (1992). These comments apply also to *T. montirivulorum* sp. nov. and *T. parastaci*. Until molecular and fine ultrastructural data become available for the type species, *T. giardi*, and other *Thelohania* species, particularly those parasitic in decapod Crustacea, the taxonomic relationships within the genus *Thelohania* are unlikely to be resolved.

It is often difficult to assign new microsporidian species to the correct genus by relying on ultrastructural or developmental features alone (Weiss and Vossbrinck 1999; Weiss 2000). Morphological features which may allow genera to be distinguished have been reviewed by Larsson (1999), however, it is easy to confuse genera, and identification based only on these features is a time consuming and difficult process. Convergent evolution of morphological features is highly probable. More than 31 microsporidian genera other than *Thelohania* have a sporogony sequence resulting in up to eight uninucleate spores within a SPV, and over 22 of these genera bud off new sporoblasts from a rosette-shaped plasmodium

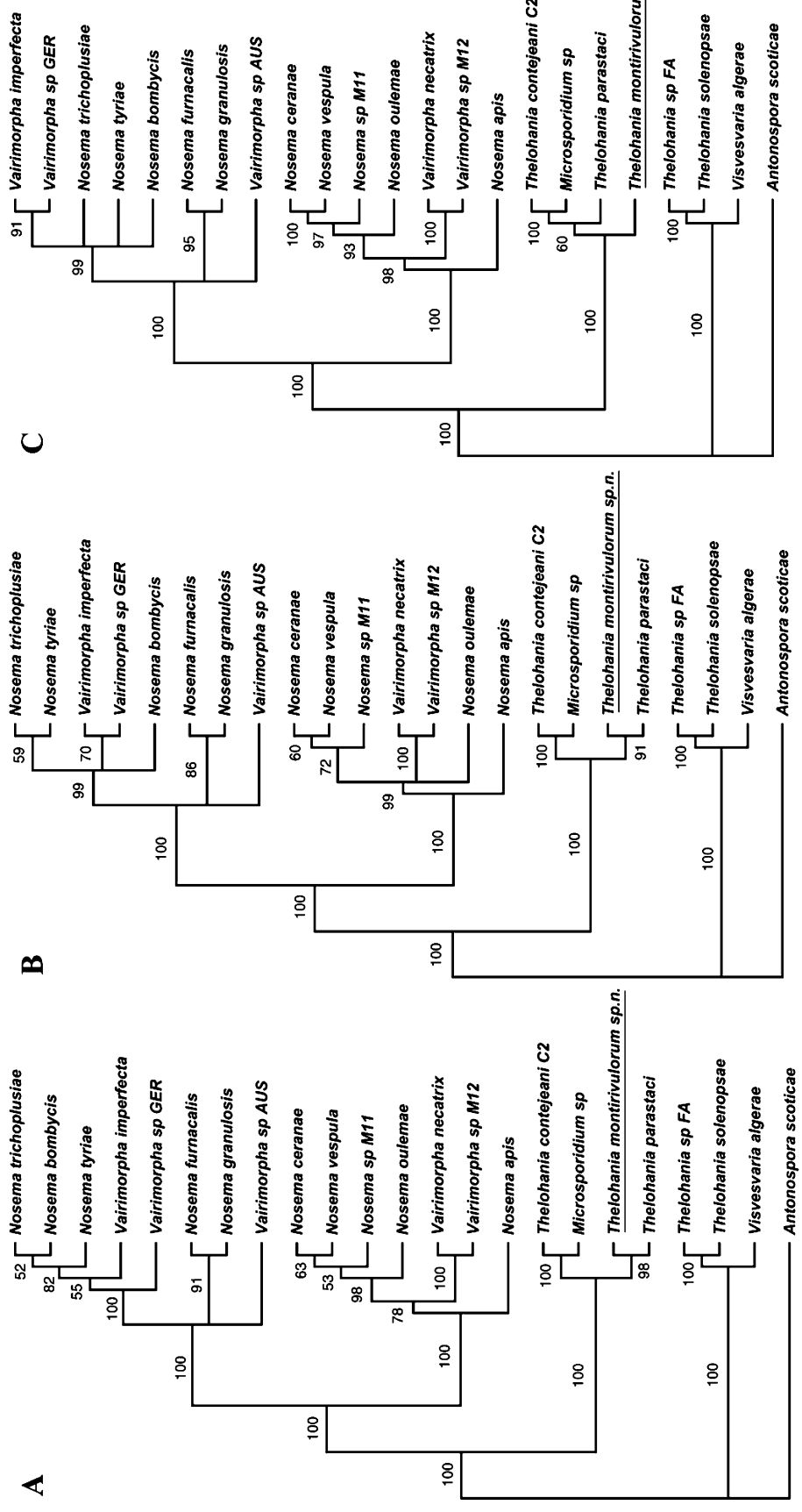
A
Nosema trichoplusiae
Nosema bombycis
Nosema tyriae
Vairimorpha imperfecta
Vairimorpha sp GER
Nosema furnacalis
Nosema granulosis
Vairimorpha sp AUS
Nosema ceranae
Nosema vespula
Nosema sp M11
Nosema oulemae
Vairimorpha necatrix
Vairimorpha sp M12
Nosema apis
Thelohania contejeani C2
Microsporidium sp
Thelohania montirivulorum sp.n.
Thelohania parastaci
Thelohania sp FA
Thelohania solenopsae
Visvesvaria algerae
Antonospora scoticae
B
Nosema trichoplusiae
Nosema tyriae
Vairimorpha imperfecta
Vairimorpha sp GER
Nosema bombycis
Nosema furnacalis
Nosema granulosis
Vairimorpha sp AUS
Nosema ceranae
Nosema vespula
Nosema sp M11
Vairimorpha necatrix
Vairimorpha sp M12
Nosema oulemae
Nosema apis
Thelohania contejeani C2
Microsporidium sp
Thelohania montirivulorum sp.n.
Thelohania parastaci
Thelohania sp FA
Thelohania solenopsae
Visvesvaria algerae
Antonospora scoticae
C
Vairimorpha imperfecta
Vairimorpha sp GER
Nosema trichoplusiae
Nosema tyriae
Nosema bombycis
Nosema furnacalis
Nosema granulosis
Vairimorpha sp AUS
Nosema ceranae
Nosema vespula
Nosema sp M11
Nosema oulemae
Vairimorpha necatrix
Vairimorpha sp M12
Nosema apis
Thelohania contejeani C2
Microsporidium sp
Thelohania parastaci
Thelohania montirivulorum sp.n.
Thelohania sp FA
Thelohania solenopsae
Visvesvaria algerae
Antonospora scoticae

Fig. 16A–C Phylogenetic trees showing relationships between SSU rDNA from *Thelohania*, *Nosema*, *Vairimorpha*, and related species. Trees were constructed using distance (**A**; GTR model), maximum parsimony (**B**) and maximum likelihood criteria (**C;** MrBayes maximum likelihood calculations). Bootstrap values >50% (10,000 repetitions) are *indicated on the branches* of trees **A** and **B**. The MrBayes maximum likelihood analysis (**C**) was based on the GTR + G model with construction of 10,000 trees (100 iterations per tree). The first 400 trees were discarded from the analysis. The frequency of observed bipartitions is *indicated on branches*. Values lower than 50% are not shown

(Larsson 1999). At least 10 genera include species that produce two or more different spore types, i.e., they form free binucleate (diplokaryotic) spores and uninucleate spores in octosporous vesicles (Canning and Vavra 2000).

By combining molecular data with ultrastructural and developmental features, it is possible to circumvent difficulties encountered with traditional taxonomy. Phylogenetic analyses based on molecular data can be performed where morphological and developmental data are inadequate or incomplete. The SSU rRNA gene is the only gene for which sequence has been obtained from a relatively wide spectrum of microsporidian species. rRNA genes are suitable candidates for phylogenetic analyses because they are found in all organisms and contain highly conserved regions, regularly interspersed with more variable regions. Phylogenetic questions at most taxonomic levels can therefore be addressed (McManus and Bowles 1996) although they are still limited by a relative paucity of data. As yet, there are no internationally defined conventions to delimit species based on molecular criteria (Kunz 2002). Over 60 *Thelohania* species that are parasites of insects (Becnel and Andreadis 1999) and at least 9 species that are parasites of crustaceans have been described (Sprague 1950; Knell et al. 1977; Lom et al. 2001; Moodie et al. 2003); SSU rDNA data was available for only 6 *Thelohania* species at the time of publication, 2 from fire ant hosts (Moser et al. 1998), 3 from

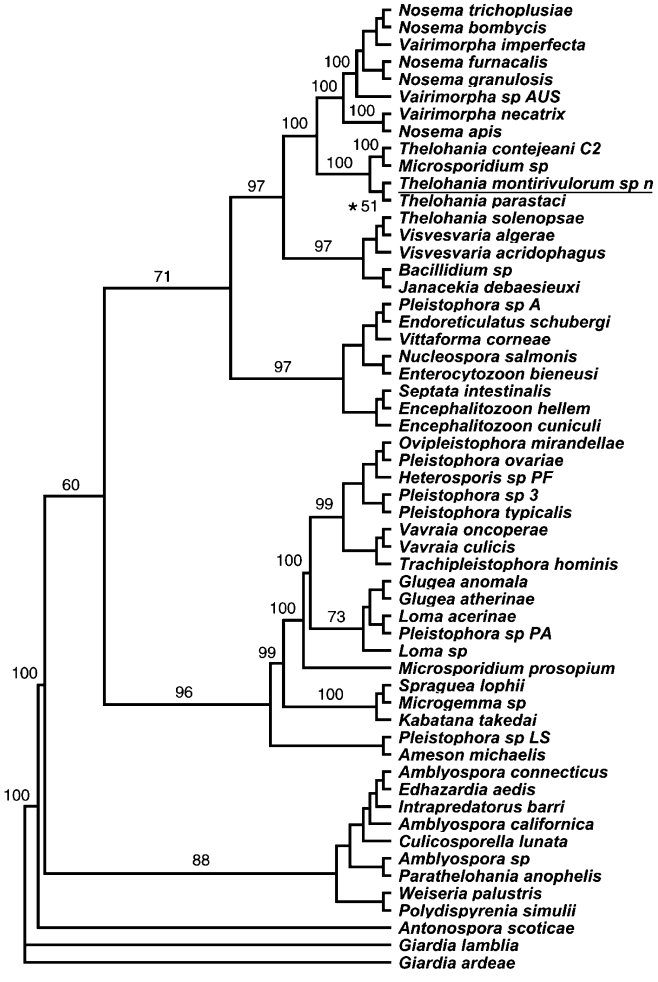

Fig. 17 Distance (NJ) tree constructed using the GTR model, showing relationships between *Thelohania* species and other genera in the phylum Microspora. Bootstrap values >50% (10,000 repetitions) are *indicated on branches* except near terminal nodes where they are omitted for clarity

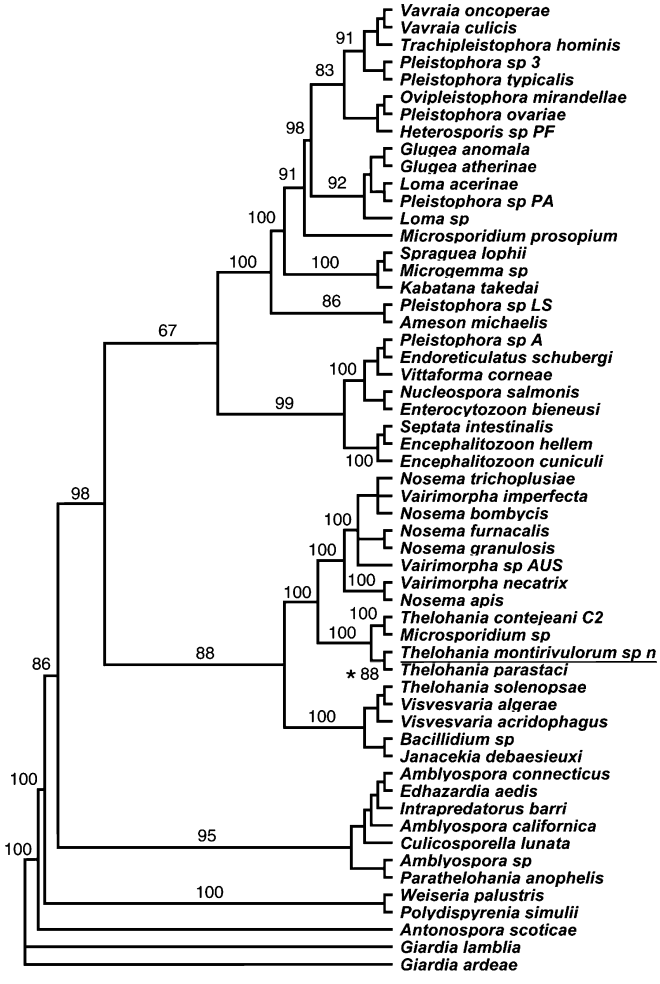

Fig. 18 Maximum parsimony consensus tree showing relationships between *Thelohania* species and other genera in the phylum Microspora. Bootstrap values >50% (10,000 repetitions) are indicated except near terminal nodes where they are omitted for clarity

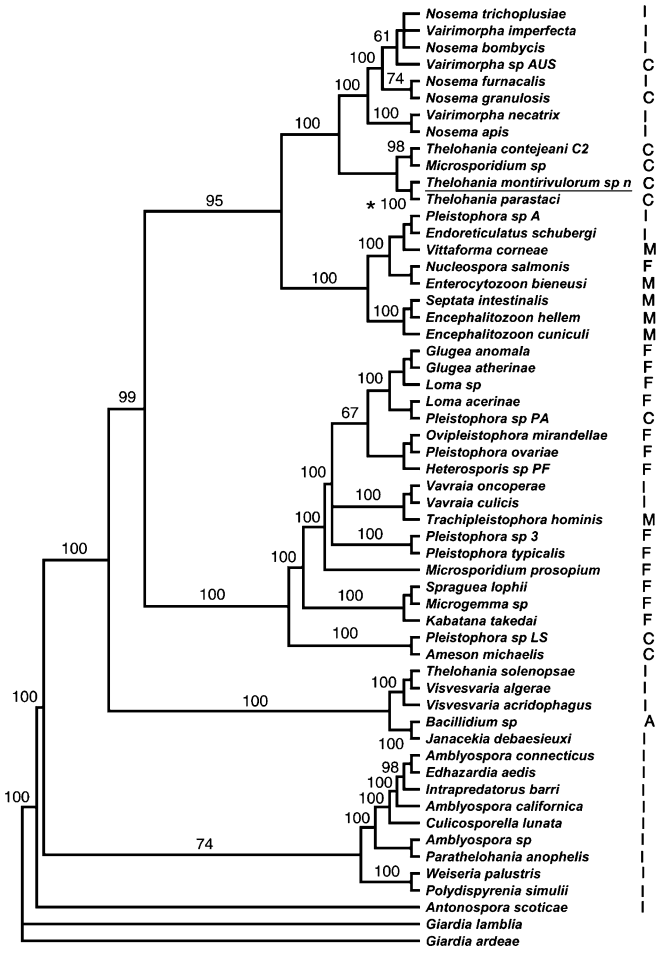

Fig. 19 MrBayes maximum likelihood consensus tree showing relationships between *Thelohania* species and other genera in the phylum Microspora. Ten thousand trees (100 iterations per tree) were constructed (GTR + G + I model), with the first 400 trees discarded from the analysis. The frequency of observed bipartitions is *indicated on branches*. Values lower than 50% are not shown. Host taxa are indicated by: *I* insect; *C* crustacean, *M* mammal, *F* fish, *A* annelid

freshwater crayfish hosts (this study; Lom et al. 2001; Moodie et al. 2003), and a probable *Thelohania* species identified as *Microsporidium* sp., from a marine amphipod, *Talorchestia deshayesei* (unpublished data, GenBank accession AJ438963).

Molecular phylogenetic analyses of a limited number of *Thelohania* species and a wide range of other species from the major lineages in the phylum Microspora (Figs. 16, 17, 18, 19) suggest that host-parasite cospeciation has occurred. In 100% of all trees in all analyses, the crayfish parasites *T. montirivulorum* sp. nov., *T. parastaci* and *T. contejeani*, from different continents in different hemispheres were grouped together in a clade that included no other microsporidian species except the undescribed European amphipod parasite *Microsporidium* sp. Members of other clades, with some exceptions, also tended to group together according to host taxa (Fig. 19), supporting the hypothesis by Baker et al. (1998) that microsporidians, e.g. the *Amblyospora* group, conform to Fahrenholz' rule, according to which parasite phylogeny mirrors host phylogeny. Lom et al. (2001) reported the same phenomenon in their analysis of 49 microsporidian species from five main lineages.

Conclusions common to the present study and the study of Lom et al. (2001) are that *Antonospora scoticae* forms the most basal branch in microsporidian trees based on SSU rDNA analysis, the *Amblyospora* group is the next to branch off after *A. scoticae*, and the clade containing *Thelohania* parasites of crayfish cannot be unambiguously placed in the tree with respect to genera other than *Vairimorpha* and *Nosema*, due to low bootstrap or bipartition frequency values. In contrast to Lom et al. (2001), *Thelohania* parasites of crustaceans were invariably placed in a sister clade to the *Vairimorpha*/*Nosema* group in the present study. *Vairimorpha* and *Nosema* species were distributed across two sub-clades in the same way as described by Canning et al. (1999), indicating that the two genera cannot be well separated. This study indicates that *Thelohania* parasites of crustacean hosts are more closely related to the *Vairimorpha*/*Nosema* clade of species from insect and crustacean hosts than to the fire ant parasites, *T. solenopsae and Thelohania* sp. Analysis of additional genes and a greater number of closely related taxa may help resolve ambiguous relationships, including those between *T. montirivulorum* sp. nov., *T. parastaci* and *T. contejeani*. Maximum likelihood, parsimony and distance methods of phylogenetic tree construction are sensitive to the number of taxa included in the analyses, in descending order of sensitivity (Siddall and Whiting 1999).

T. montirivulorum sp. nov. and *T. parastaci* are found in crayfish from the superfamily Parastacoidea, whereas *T. contejeani* is found in crayfish from the superfamily Astacoidea. Recent research on the evolution of freshwater crayfish tends to support a monophyletic origin, probably from a marine ancestor. Clear separation between the crayfish superfamilies Parastacoidea and Astacoidea is thought to have occurred at least 185–225 million years ago, before the supercontinent Pangaea broke up (Crandall 2002). Molecular data from a wider range of *Thelohania* species parasitic in freshwater and marine decapods is required to address the question of precisely how *Thelohania* species co-evolved with their crayfish hosts. Ideally, phylogenetic inferences should be based on more than one gene, so that relationships can be corroborated with evidence from several sources, and molecular phylogenies of both host and parasite taxa studied in tandem.

The microsporidian parasites of Australia's diverse freshwater crayfish fauna have not been well studied. Further research employing molecular and classical methods of taxonomy should throw light on the phylogenetic relationships and biogeographical features of this interesting group of parasites. The functions of the different spore types in the life cycles of *Thelohania* parasites of crustaceans have yet to be determined and it is hoped that the SSU and ITS rDNA sequences

presented in this study will facilitate the use of molecular techniques, e.g. PCR or in situ hybridisation, to elucidate transmission pathways and other life cycle features of *T. montirivulorum* sp. nov., and related species.

Taxonomic summary—*Thelohania montirivulorum* sp. nov.

Type host The freshwater crayfish *Cherax destructor destructor* (Austin 1996).

Transmission Unknown.

Site of infection Muscle tissue of adult crayfish.

Host-parasite interface Uninucleate spores produced in sporophorous vesicles of parasite origin. Early sporonts and diplokaryotic spores in direct contact with host cell cytoplasm.

Merogony Early meronts and their mode of division not observed.

Transition to sporogony Sporonts round in shape, diplokaryotic and identified by thickening of parasite plasmalemma with highly vacuolated/vesicular cytoplasm.

Sporogony Simultaneous dimorphic sporogony in muscle tissue. One sporogony pathway involves binary fission with production of diplokaryotic spores in contact with host cell cytoplasm. The other sporogony pathway involves formation of a sporophorous vesicle with production of up to eight uninucleate spores per vesicle, presumably by meiosis.

Binucleate spores Diplokaryotic. Lozenge shaped, variable in size. Average fresh spore length: 5.9 (4.9–7.2) μm. Average fresh spore width: 2.6 (2.0–3.1) μm. Isofilar polar filament with 20–22 coils, 107 (90–140) nm in diameter. Lamellar polaroplast. Lateral exospore width: 22 (17–30) nm. Lateral endospore width: 65 (40–80) nm.

Uninucleate spores Develop from a rosette shaped plasmodium inside sporophorous vesicle. Lozenge shaped. Isofilar polar filament with 20–22 coils, 98 (82–111) nm in diameter. Lateral exospore width: 31 (30–40) nm. Lateral endospore width: 108 (80–130) nm.

Sporophorous vesicles Of parasite origin. Average vesicle diameter 8.4 (7.0–9.6) μm. 2 to 8 spores per vesicle. Contain macrotubules: 171 (130–249) nm in diameter, microtubules: 85 (63–117) nm in diameter, and early in sporoblast development, granular dense bodies.

Type locality Upper Gwydir River catchment: Tea Tree Creek, 20 km west of Armidale, NSW, Australia (30° 30′ S, 151° 29′ E).

Type specimens Giemsa stained smears were submitted to the Queensland Museum, Brisbane, Australia. Hapantotype submission number: G463713. Parahapantotype submission number: G463714.

Molecular data 16S SSU rDNA gene cloned and sequenced, Genbank accession number: AY183664. ITS rDNA region directly sequenced, Genbank, accession number: AY183665.

Remarks The descriptor *montirivulorum* is derived from Latin and refers to the mountain stream from which this species was collected. Many spores were imperfectly formed. Phylogenetic studies based on SSU rDNA sequences indicate this species is closely related to *T. parastaci* and *T. contejeani*.

Acknowledgements This research was supported by a joint scholarship from the University of New England and CSIRO, Livestock Industries. The authors particularly wish to thank the following people for their assistance: Dr. Robert Adlard, Dr. Carlos Azevedo, Dr. Jeremy Bruhl, Prof. Iva Dykova, Mr. Zoltan Enoch, Mr. Peter Garlick, Prof. Robin Gasser, Dr. Dean Jerry, Ms. Mahri Koch, Mr. Ian Lenane, Mr. Callum Mack, Dr. Jennifer Mathews, Dr. Mary Notestine, Dr. Peter O'Donoghue, Prof. Klaus Rohde, Dr. Jessica Worthington-Wilmer, and Dr. Tony Sweeney.

References

Austin CM (1996) Systematics of the freshwater crayfish genus *Cherax* Erichson (Decapoda: Parastacidae) in northern and eastern Australia: electrophoretic and morphological variation. Aust J Zool 44:259–296

Baker MD, Vossbrinck CR, Becnel JJ, Andreadis TG (1998) Phylogeny of Amblyospora (Microsporida: Amblyosporidae) and related genera based on small subunit ribosomal DNA data: a possible example of host parasite cospeciation. J Invertebr Pathol 71:199–206

Becnel JJ, Andreadis TG (1999) Microsporidia in insects. In: Wittner M, Weiss LM (eds) The Microsporidia and Microsporidiosis. ASM, Washington, D.C., pp 447–501

Canning EU, Vavra J (2000) Phylum Microsporida. In: Lee JJ, Leedale GF (eds) An illustrated guide to the Protozoa, 2nd edn. Society of Protozoologists, Lawrence, Kan., pp 39–126

Canning EU, Curry A, Cheney S, Lafranchi-Tristem NJ, Haque MA (1999) *Vairimorpha imperfecta* n.sp., a microsporidian exhibiting an abortive octosporous sporogony in *Plutella xylostella* L. (Lepidoptera: Yponomeutidae). Parasitology 119:273–286

Cossins AR, Bowler K (1974) An histological and ultrastructural study of *Thelohania contejeani* Henneguy, 1892 (Nosematidae), microsporidian parasite of *Austropotamobius pallipes* Lereboullet. Parasitology 68:81–91

Crandall KA (2002) Crayfish as model organisms. Freshw Crayfish 13:3–10

Flegel TW, Pasharawipas T (1995) A proposal for typical eukaryotic meiosis in microsporidians. Can J Microbiol 41:1–11

France RL, Graham L (1985) Increased microsporidian parasitism of the crayfish *Orconectes virilis* in an experimentally acidified lake. Water Air Soil Pollut 25:129–136

Huelsenbeck JP, Ronquist F (2001) MRBAYES: Bayesian inference of phylogenetic trees. Bioinformatics 17:754–755

Jeanmougin F, Thompson JD, Gouy M, Higgins DG, Gibson TJ (1998) Multiple sequence alignment with Clustal X. Trends Biochem Sci 23:403–405

Jones JB, Lawrence CS (2001) Diseases of yabbies (*Cherax albidus*) in Western Australia. Aquaculture 194:221–232

Knell JD, Allen GE, Hazard EI (1977) Light and electron microscope study of *Thelohania solenopsae* n. sp. (Microsporida: Protozoa) in the red imported Fire Ant, *Solenopsis invicta*. J Invertebr Pathol 29:192–200

Kunz W (2002) When is a parasite species a species? Trends Parasitol 18:121–124

Lanave C, Preparata G, Saccone C, Serio G (1984) A new method for calculating evolutionary substitution rates. J Mol Evol 20:86–93

Langdon JS (1991) Microsporidiosis due to a pleistophorid in marron, *Cherax tenuimanus* (Smith), (Decapoda: Parastacidae). J Fish Dis 14:33–44

Larsson JIR (1999) Identification of microsporidia (review). Acta Protozool 38:161–197

Lom J, Nilsen F, Dykova I (2001) *Thelohania contejeani* Henneguy, 1892: dimorphic life cycle and taxonomic affinities, as indicated by ultrastructural and molecular study. Parasitol Res 87:860–872

McManus DP, Bowles J (1996) Molecular genetic approaches to parasite identification: their value in diagnostic parasitology and systematics. Int J Parasitol 26:687–704

Moodie EG, Le Jambre LF, Katz ME (2003) *Thelohania parastaci* sp. nov. (Microspora: Thelohaniidae), a parasite of the Australian freshwater crayfish, *Cherax destructor* (Decapoda: Parastacidae). Parasitol Res (in press)

Moser BA, Becnel JJ, Maruniak J, Patterson RS (1998) Analysis of the ribosomal DNA sequences of the microsporidia *Thelohania* and *Vairimorpha* of Fire Ants. J Invertebr Pathol 72:154–159

Nylund V, Westman K (1992) Crayfish diseases and their control in Finland. Finn Fish Res 14:107–118

O'Donoghue PJ, Adlard RD (2000) Catalogue of protozoan parasites recorded in Australia. In: Memoirs of the Queensland Museum. Queensland Museum, Brisbane, Australia, 45:1–163

O'Donoghue P, Beveridge I, Phillips P (1990) Parasites and ectocommensals of yabbies and marron in South Australia. Central Veterinary Laboratories (VETLAB), South Australian Department of Agriculture, Adelaide

Page RDM, Holmes EC (1998) Molecular evolution: a phylogenetic approach. Blackwell, Oxford

Posada D, Crandall KA (1998) MODELTEST: testing the model of DNA substitution. Bioinformatics 14:817–818

Quilter CG (1976) Microsporidian parasite *Thelohania contejeani* Henneguy from New Zealand freshwater crayfish. NZ J Mar Freshw Res 10:225–231

Rodriguez R, Oliver JL, Marin A, Medina JR (1990) The general stochastic model of nucleotide substitution. J Theor Biol 142:485–501

Siddall ME, Whiting MF (1999) Long-branch abstractions. Cladistics 15:9–24

Sprague V (1950) *Thelohania cambari* n. sp., a microsporidian parasite of North American crayfish. J Parasitol [Suppl] 36:46

Sprague V, Becnel JJ, Hazard EJ (1992) Taxonomy of Phylum Microspora. Crit Rev Microbiol 18:285–395

Swofford DL (2000) PAUP*. Phylogenetic analysis using parsimony (*and other methods), vers 4. Sinauer, Sunderland, Mass.

Thompson JD, Higgins DG, Gibson TJ (1994) Clustal W: improving the sensitivity of progressive multiple sequence alignment through sequence weighting, position-specific gap penalties and weight matrix choice. Nucleic Acids Res 22:4673–4680

Undeen A (1997) Microsporidia (Protozoa): a handbook of biology and research techniques. Center for Medical, Agricultural and Veterinary Entomology, Gainesville, Fla. http://www.okstate.edu/OSU_Ag/agedcm4 h/ag_news/SCSB387.htm

Vivares CP (1975) Etude comparative faite en microscopies photonique et electronique de trois especes de microsporidies appartenant au genre *Thelohania* Henneguy, 1892, parasites de crustaces decapodes marins. Ann Sci Nat Zool Paris 17:141–178

Vivares CP (1980) An ultrastructural study of *Thelohania maenadis* Perez (Microspora, Microsporidia) and new facts on the genus *Thelohania* Henneguy. Arch Protistenkd 123:44–60

Weiss LM (2000) Molecular phylogeny and diagnostic approaches to Microsporidia. In: Petry F (ed) Cryptosporidiosis and microsporidiosis. Karger, Basel, pp 209–235

Weiss LM, Vossbrinck CR (1998) Microsporidiosis: molecular and diagnostic aspects. In: Tzipori S (ed) Opportunistic Protozoa in humans. Academic Press, London, pp 351–395

Weiss LM, Vossbrinck CR (1999) Molecular biology, molecular phylogeny, and molecular diagnostic approaches to the Microsporidia. In: Wittner M, Weiss LM (eds) The Microsporidia and Microsporidiosis. ASM Press, Washington, D.C., pp 129–171